



Oligothiophene based small molecules with a new end group for solution processed organic photovoltaics



Huijing Zhang, Xuan Yang, Nailiang Qiu, Wang Ni, Qian Zhang, Miaomiao Li, Bin Kan, Xiangjian Wan, Chenxi Li, Yongsheng Chen*

Key Laboratory of Functional Polymer Materials, Collaborative Innovation Center of Chemical Science and Engineering (Tianjin), Center for Nanoscale Science and Technology, Institute of Polymer Chemistry, College of Chemistry, Nankai University, Tianjin 300071, China

ARTICLE INFO

Article history:

Received 7 December 2015
Received in revised form
1 March 2016
Accepted 9 March 2016

Keywords:

Small molecule
Organic photovoltaic cell
Solvent vapor annealing
Low band gap

ABSTRACT

Two oligothiophene based small molecules (**DINER5T** and **DINER7T**) with a new end group **INER** were synthesized as the donors for organic solar cells, and their photovoltaic performance was studied and compared with the corresponding compounds (**DRHD7T** and **DIN7T**) with the same backbone structure but different end groups. Both of the new molecules exhibit broad and red shift absorption compared with **DRHD7T** and **DIN7T**, with very low band gaps of 1.47 eV and 1.34 eV, respectively. The devices based on **DINER5T**:PC₇₁BM and **DINER7T**:PC₇₁BM blend films gave PCEs of 4.22% and 4.02%, respectively, through a solvent vapor annealing (SVA) process with CH₂Cl₂.

© 2016 Published by Elsevier B.V.

1. Introduction

Organic photovoltaic devices (OPVs) due to their advantages, such as low cost and flexibility, have caught ever growing attention. The power conversion efficiencies (PCEs) of OPVs are increasing quickly and PCEs over 10% have been achieved for both polymer based OPVs (P-OPVs) [1–9] and small molecule based OPVs (SM-OPVs) [10–12]. Based on the equation, $PCE = V_{oc} \times J_{sc} \times FF / P_{in}$, where V_{oc} is the open-circuit voltage, J_{sc} is the short-circuit current density, FF is the fill factor and P_{in} is the incident light intensity, both V_{oc} and FF of the devices have been improved drastically recently, thus one of the current focuses is to enhance J_{sc} for better performance. To get a high J_{sc} , several effective methods have been widely used. For example, morphology control by thermal [13–15] or vapor annealing [16–19], adding additives [20–24], modifying buffer layer [25], introducing metal nano particles [26,27] et al., have been used widely. But the most and fundamental strategy is still to design low band gap molecules to harvest solar light as much as possible, thus more solar energy could be theoretically converted into electric energy.

Oligothiophene based small molecules, due to their relative easy

synthesis and purification, good solubility and outstanding photoelectricity properties, have been widely used in organic solar cells [28–30], dye-sensitized solar cell [31,32], and perovskite solar cells [33]. Besides, their electrochemical properties and crystalline nature could be easily modulated, which makes this kind of molecules catch increasing attention [34,35]. Recent years, we have reported a series of oligothiophene based small molecules with Acceptor-Donor-Acceptor (A-D-A) structures for high efficient organic solar cells [10,12,36,37], and >10% PCE has been achieved [12]. It has been found that the electron withdrawing end groups played a great role on the molecules' absorption, energy levels, solid state packing modes and the final device performance. Among the end groups used for these oligothiophene-like small molecules, the rhodanine unit turns out to be an excellent choice as in the case of DERHD7T which shows excellent absorption in the range from 400 to 800 nm [38]. Thus, device based on DERHD7T gave high J_{sc} over 13 mA/cm². However, the device with DERHD7T as the donor exhibited a low FF of around 47%. On the other hand, the molecule DIN7T with indandione end groups showed broad absorption and a high FF over 0.70. However, its devices gave a lower J_{sc} of 8.21 mA/cm² [39]. Obviously, the big difference on the corresponding devices performance of the two small molecules were caused by the end groups that would lead to different energy levels and morphology of the active layers. Thus, it is rather desirable to design new donor molecules using these different end groups to combine their

* Corresponding author.

E-mail address: yschen99@nankai.edu.cn (Y. Chen).

advantages.

So, herein, a new end group, named **INER**, was designed and two new donor molecules named **DINER5T** and **DINER7T** were synthesized (Scheme 1) using this new end group. Compared with the two previous molecules of DERHD7T and DIN7T, the absorption of the two new molecules were greatly improved with a maximum absorption peak at 664 nm for **DINER7T**, and 680 nm for **DINER5T**, respectively. Devices fabricated using these two molecules as donors and PC₇₁BM as the acceptor were systematically investigated via adding additives and solvent vapor annealing (SVA) optimization. PCEs of 4.02% and 4.22% were achieved for **DINER7T** and **DINER5T** based devices, respectively. The moderate efficiencies are thought to be caused by the unfavorable planarity of the two molecules and unsuitable phase separation scale.

2. Experimental section

2.1. Materials and synthesis

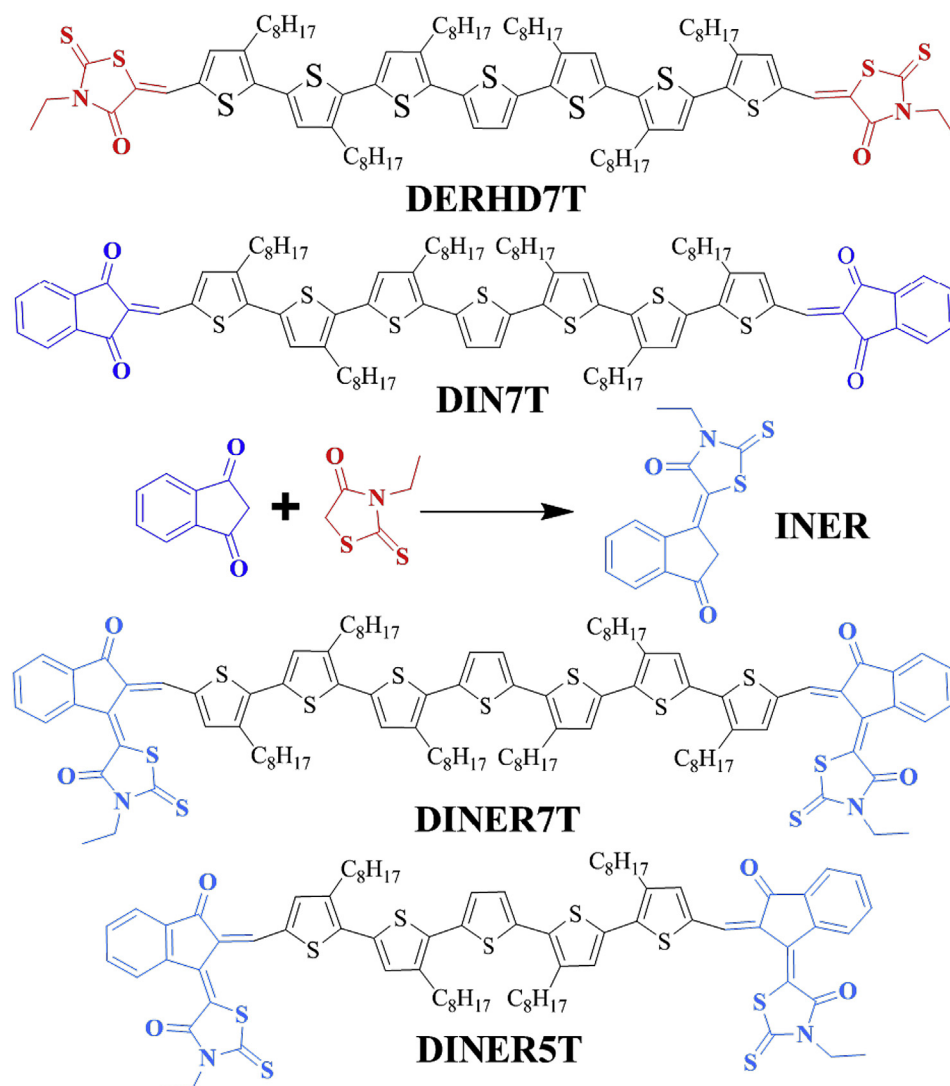
All reactions and manipulations were carried out under argon atmosphere with the use of standard Schlenk techniques. Unless otherwise specified, all the starting materials were purchased from

commercial suppliers and used directly without any purification. Compounds DF5T and DF7T were synthesized according to the literature [30]. The procedure of synthesis of **INER**, **DINER5T** and **DINER7T** is outlined in Scheme 2.

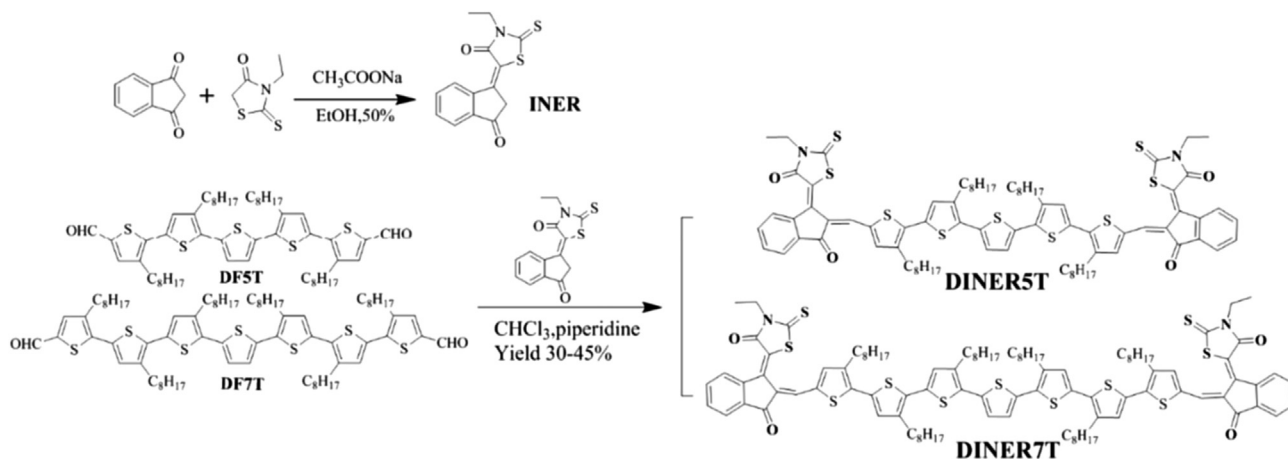
2.2. Synthesis of compound **INER**, **DINER5T** and **DINER7T**

2.2.1. Synthesis of compound **INER**

Indandione (146 mg, 1 mmol) and 3-ethylrhodanine (161 mg, 1 mmol) were dissolved in absolute ethanol (50 mL), then 30 mg CH₃COONa was added and the resulted solution were stirred for 30 h at 65–70 °C under argon. After removal of the solvent, the crude product was dissolved with chloroform and separated by chromatography using silica gel and a mixture of dichloromethane and petroleum ether (2: 1) as eluent to afford **INER** as a yellow solid (145 mg, 50% yield). ¹H NMR (400 MHz, CDCl₃): δ 7.95 (d, 1H), 7.85 (t, 1H), 7.80 (d, 1H), 7.68 (t, 1H), 4.22 (m, 2H), 3.95 (s, 2H), 1.31 (t, 3H). ¹³C NMR (100 MHz, CDCl₃): δ 200.54, 191.64, 166.71, 146.28, 139.10, 139.03, 135.47, 131.98, 126.19, 124.49, 118.27, 43.35, 39.82, 12.27. MS (EI) *m/z* calcd. for C₁₄H₁₁NO₂S₂ [M⁺], 289.37, Found, 288.0.



Scheme 1. The chemical structures of DERHD7T, DIN7T, **INER**, **DINER7T** and **DINER5T**.



Scheme 2. The synthesis routes to **DINER5T** and **DINER7T**.

2.2.2. Synthesis of compound **DINER5T**

DF5T (400 mg, 0.44 mmol) and **INER** (1270 mg, 4.4 mmol) was dissolved in a solution of dry chloroform (100 mL). Then three drops of piperidine was added and the resulted solution was stirred for 36 h at 60 °C under argon. After removal the solvent, the crude product was precipitated from acetone and the precipitate was filtered off. The procedure was repeated for several times. Then the precipitate was dissolved in chloroform and precipitated from hexane, the precipitate was filtered off, the procedure was repeated for several times. Finally, the product was separated by chromatography using silica gel and a mixture of dichloromethane and hexane (1.5:1) as eluent to afford **DINER5T** as a black solid (200 mg, 31% yield). ¹H NMR (400 MHz, CDCl₃): δ 9.33 (d, 1H), 9.23 (d, 1H), 7.94 (t, 2H), 7.90 (d, 1H), 7.72 (m, 3H), 7.61 (m, 3H), 7.53 (d, 1H), 7.31 (s, 2H), 7.16 (s, 2H), 4.26 (m, 4H), 2.84 (d, 8H), 2.01 (m, 6H), 1.73 (m, 8H), 1.25 (m, 40H), 0.88 (d, 12H). Anal. Calcd. for C₈₂H₉₄N₂O₄S₉: C, 67.45; H, 6.49; N, 1.92. Found: C, 67.69; H, 6.12; N, 2.00. MS (MOLDI TOF) *m/z* calcd. for C₈₂H₉₄N₂O₄S₉ [M]⁺, 1458.470, Found 1458.281.

2.2.3. Synthesis of compound **DINER7T**

Diformylseptithiophene (DF7T) (400 mg, 0.31 mmol) and **INER** (895 mg, 3.1 mmol) was dissolved in a solution of dry chloroform (100 mL). Then three drops of piperidine was added and the resulting solution was stirred for 30 h at 60 °C under argon. After removal the solvent, the crude product was precipitated from acetone and the precipitate was filtered off. The procedure was repeated for several times. Then the precipitate was dissolved in chloroform and precipitated from hexane, the precipitate was filtered off, the procedure was repeated for several times. Finally, the product was separated by chromatography using silica gel and a mixture of dichloromethane and hexane (2:1) as eluent to afford **DINER7T** as a black solid (250 mg, 44% yield). ¹H NMR (400 MHz, CDCl₃): δ 9.33 (d, 1H), 9.20 (d, 1H), 7.92 (m, 3H), 7.69 (m, 3H), 7.58 (m, 4H), 7.24 (s, 2H), 7.15–7.10 (m, 2H), 7.06–7.01 (d, 2H), 4.27 (m, 4H), 2.82 (m, 12H), 1.71 (m, 6H), 1.31 (m, 60H), 0.89 (d, 18H). Anal. Calcd. for C₈₂H₉₄N₂O₄S₉: C, 68.86; H, 7.09; N, 1.52. Found: C, 68.42; H, 7.14; N, 1.61. MS (MOLDI TOF) *m/z* calcd. for C₁₀₆H₁₃₀N₂O₄S₁₁ [M]⁺, 1847.699, Found 1847.915.

2.3. Instruments and measurements

Nuclear magnetic resonance (¹H NMR and ¹³C NMR) spectra were taken on a Bruker AV400 Spectrometer. MALDI-TOF spectra were performed on a Bruker Autoflex III instrument. UV–Vis spectra were obtained with a JASCO V-570 spectrophotometer. The

organic molecule films on quartz used for absorption spectral measurement were prepared by spin-coating their chloroform solutions. Cyclic voltammetry (CV) experiments were performed with a LK98B II microcomputer-based electrochemical analyzer in CH₂Cl₂ solutions which were carried out at room temperature employing a glassy carbon electrode as the working electrode, a saturated calomel electrode (SCE) as the reference electrode, and a Pt wire as the counter electrode. Dichloromethane was distilled from calcium hydride under dry nitrogen immediately prior to use. Tetrabutylammonium phosphorus hexafluoride (Bu₄NPF₆ 0.1 M) in dichloromethane was used as the supporting electrolyte, and the scanning rate was 100 mV s⁻¹. Atomic force microscope (AFM) investigation was performed using Bruker Multi Mode 8 in “tapping” mode. The transmission electron microscope (TEM) investigation was performed on a Philips Technical G2 F20 at 200 kV. SCLC mobility was measured using a diode configuration of ITO/PEDOT:PSS/donor:PC₇₁BM or neat donor/Au for hole and Al/active layer/Al for electron by taking the dark current density in the range of 0–8 V and fitting the results to a space charge limited form, where SCLC is described by:

$$J = \frac{9\epsilon_0\epsilon_r\mu_0V^2}{8L^3} \exp\left(0.89\sqrt{\frac{V}{L}}\right)$$

where *J* is the current density, *L* is the film thickness of the active layer, μ_0 is the hole mobility, ϵ_r is the relative dielectric constant of the transport medium, ϵ_0 is the permittivity of free space (8.85×10^{-12} Fm⁻¹), *V* (=V_{appl}–V_{bi}) is the internal voltage of the device, V_{appl} is the applied voltage to the device and V_{bi} is the built-in voltage due to the relative work function difference of the two electrodes.

The current density–voltage (*J*–*V*) characteristics of photovoltaic devices were obtained by a Keithley 2400 source-measure unit. The photocurrent was measured under illumination simulated 100 mWcm⁻² AM1.5G irradiation using axenon-lamp-based solar simulator [SAN-EI XES-70S1] in an argon filled glove box. Simulator irradiance was characterized using a calibrated spectrometer and illumination intensity was set using a certified silicon diode. External quantum efficiency (EQE) value of the encapsulated device was obtained with a halogen-tungsten lamp, monochromator, optical chopper, and lock-in amplifier in air and photon flux was determined by a calibrated silicon photodiode.

2.4. Fabrication of photovoltaic devices

The photovoltaic devices were fabricated with a structure of glass/ITO/PEDOT:PSS/Donor:Acceptor/ZnO/Al. The ITO coated glass substrates were cleaned by detergent, deionized water, acetone, and isopropyl alcohol under ultrasonication for 15 min each time and then dried by a nitrogen blow. PEDOT:PSS layer was spin-coated (3000 rpm, ca. 40 nm thick) onto the cleaned ITO surface. The substrates were then placed into an argon-filled glove box after being baked at 150 °C for 20 min. Subsequently, the active layer was spin-coated from donor (8 mg mL⁻¹) and PC₇₁BM in chloroform solution at 1700 rpm for 20 s on the ITO/PEDOT:PSS substrate. The active layer thickness was measured using a Dektak150 profilometer. Afterward, ZnO particle suspension was spin-coated at 3000 rpm on the active layer and finally, a 50 nm Al layer were deposited on the ZnO layer under high vacuum ($<1.5 \times 10^{-4}$ Pa). The effective area of each cell was 4 mm², defined by masks for all the solar cell devices discussed in this work.

3. Results and discussion

3.1. Optical and electrochemical properties

The UV-Vis absorption spectra of **DINER7T** and **DINER5T** in chloroform solution and on solid films prepared by spin coating are shown in Fig. 1. The important optical absorption data and electrochemistry data of these two new molecules, compared with those of DERHD7T and DIN7T, are summarized in Table 1.

As listed in Table 1, compared with the absorption of DERHD7T and DIN7T, both of **DINER5T** and **DINER7T** have a large red-shift of about 40–80 nm, with a narrow optical band gap of 1.37 and 1.45 eV, respectively. Fig. 1 demonstrated that the absorption of the two molecules covered a wide range from 400 to nearly 900 nm, indicating that the incorporation of **INER** can largely broaden the absorption of the oligothiophene small molecules as expected.

3.2. Photovoltaic properties

Bulk heterojunction (BHJ) solar cells were fabricated using **DINER7T** and **DINER5T** as the electron donor with a conventional device structure of ITO/PEDOT:PSS/**DINER7T** or **DINER5T**: PC₇₁BM/ZnO/Al. Without any treatment, the devices based on the two small molecules gave poor PCEs, 1.39% for **DINER7T** and 1.12% for

DINER5T, respectively. To optimize the performance of the devices, several additives were used. However, no clear improvement was observed (Table S1). Then, the solvent vapor annealing strategy developed recently [17] was used to optimize the devices. The photovoltaic parameters with different solvents for SVA were listed in Table 2. Among the solvents used for SVA, CH₂Cl₂ gave the best device performances with PCEs of 4.02% and 4.22% for **DINER7T** and **DINER5T**, respectively. The J-V curves of the two molecules based devices (with/without CH₂Cl₂ SVA) were shown in Fig. 2.

To investigate the influence of SVA with CH₂Cl₂ on the device performance, UV-Vis absorption spectra of blend films (as casted and SVA treated) and external quantum efficiency (EQE) were measured. As shown in Fig. 3, when pure films were treated with CH₂Cl₂, the absorption exhibited about 5–10 nm red shift and absorption region got broader. While, when blended with PC₇₁BM, the maximum absorption peaks of both **DINER5T** and **DINER7T** exhibited almost 50 nm blue shift. Then after annealing with CH₂Cl₂, the absorption red shifted again and the absorption spectra became broadened also. This phenomenon reveals that when blended with PC₇₁BM, the crystallinity of **DINER5T** and **DINER7T** would be weakened but can be improved by SVA treatment. The EQE curves (Fig. 4) demonstrated that the EQE increased evidently after SVA compared with the devices without SVA. Especially, **DINER5T** based devices is more sensitive to the SVA treatment than that of **DINER7T** based devices, and the EQE increased drastically within almost all the absorption region.

The morphologies of **DINER5T**:PC₇₁BM and **DINER7T**:PC₇₁BM blend films were investigated by AFM and TEM. As shown in Fig. S2, the root mean square (RMS) roughness values are 0.396 and 0.412 nm for **DINER5T**:PC₇₁BM and **DINER7T**:PC₇₁BM blend films without SVA treatment. While when the blend films were treated with CH₂Cl₂, the RMS roughness increased to 0.916 and 0.635 nm for **DINER5T**:PC₇₁BM and **DINER7T**:PC₇₁BM blend films, respectively, indicating enlarged phase separation scale. The same phenomenon was observed in TEM images as shown in Fig. 5. As can be seen from the TEM images, both of the two molecules show good miscibility with PC₇₁BM, without apparent phase separation between donor phase and acceptor phase presented. Post-treatment of solvent vapor annealing resulted in the formation of network of nano-rods, with similar diameters of 40–60 nm in both blend films. The increased intermolecular packing and formation of interpenetration network could facilitate the separation of excitons and the transportation of mobile carriers, which is consistent with the enhanced device performance. The relatively wide diameters, however, limit exciton diffusion/dissociation efficiency, resulting in the moderate device performances. Some bright particles observed in **DINER7T**:PC₇₁BM blend film after post-treatment indicate some over aggregation of **DINER7T** phase, which results in lower J_{sc} than that of **DINER5T**. The results are consistent with the mobility analysis of the small molecules based devices. After the SVA treatment with CH₂Cl₂, the hole mobility increased from 8.51×10^{-5} and 6.84×10^{-5} cm² V⁻¹ S⁻¹ to 2.90×10^{-4} and 1.82×10^{-4} cm² V⁻¹ S⁻¹ for **DINER5T** and **DINER7T** based devices, respectively. In accordance with hole mobility, after SVA treatment with CH₂Cl₂, the electron mobility was improved from 6.51×10^{-5} and 6.46×10^{-5} cm² V⁻¹ S⁻¹ to 1.74×10^{-4} and 1.61×10^{-4} cm² V⁻¹ S⁻¹ for **DINER5T** and **DINER7T** based devices, respectively. The corresponding Figure were shown in Fig. S3 and S4. However, surprisingly, the ordered donor phase turned out to be nano-rods, not the optimized nano fibers (ideally with diameters of 10–15 nm) as observed before for a better performance [10], though many methods have been tested. Thus, this might be the main factor for the limited PCEs of the devices based on **DINER5T** and **DINER7T**.

We calculated the molecular geometries of the two molecules

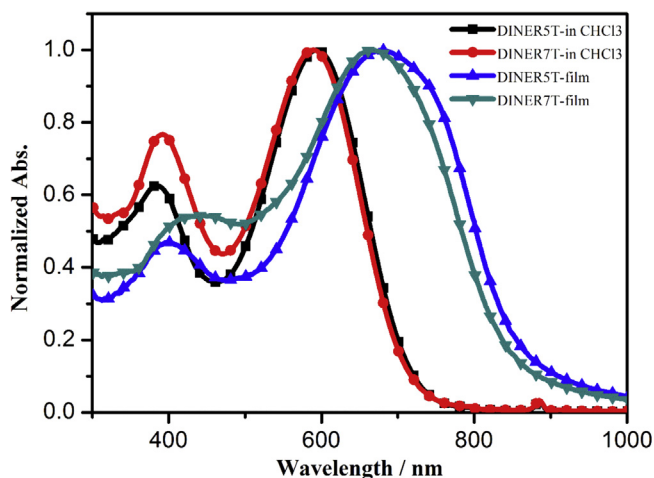


Fig. 1. Absorption spectra of **DINER5T** and **DINER7T** in chloroform solution and as cast film.

Table 1
Optical and electrochemical data of **DINER7T**, **DINER5T**, **DERHD7T** and **DIN7T**.

Compounds	λ_{\max} solution (nm)	λ_{\max} film (nm)	E_g^{opt} film (eV)	E_g^{v} (eV)	HOMO (eV)	LUMO (eV)
DINER7T	588	664	1.37	1.34	−4.93	−3.59
DINER5T	590	680	1.45	1.47	−5.03	−3.56
DERHD7T^a	508	618	1.69	1.72	−4.97	−3.44
DIN7T^b	541	630	1.49	1.53	−5.02	−3.72

^a Data from Ref. [30].

^b Data from Ref. [31].

Table 2
Influence of SVA with different solvents on device performance.

Donor	Solvents	V_{oc}/V	$J_{sc}/(\text{mA cm}^{-2})$	FF	PCE/%
DINER7T	As cast	0.91	5.30	0.29	1.39
	THF	0.85	4.28	0.27	0.98
	CHCl_3	0.87	4.98	0.31	1.34
	CS_2	0.79	6.09	0.39	1.87
	CH_2Cl_2	0.84	8.56	0.56	4.02
DINER5T	As cast	0.93	4.67	0.26	1.12
	THF	0.91	4.47	0.30	1.22
	CHCl_3	0.91	6.38	0.28	1.62
	CS_2	0.83	4.49	0.45	1.67
	CH_2Cl_2	0.88	10.21	0.47	4.22

SVA time: 60s.

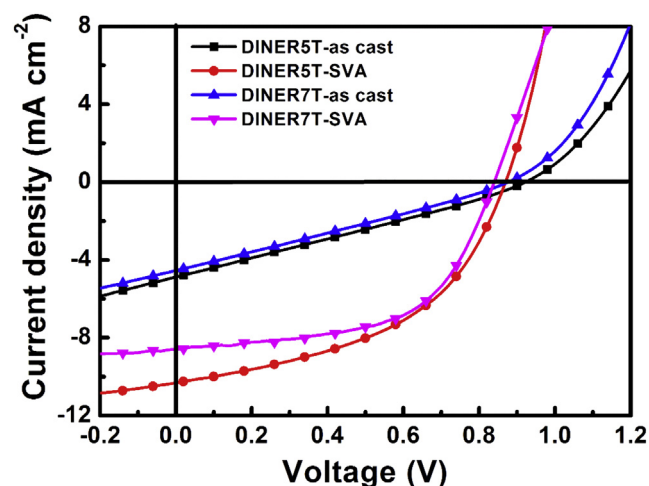


Fig. 2. J-V curves of **DINER5T** and **DINER7T** based devices.

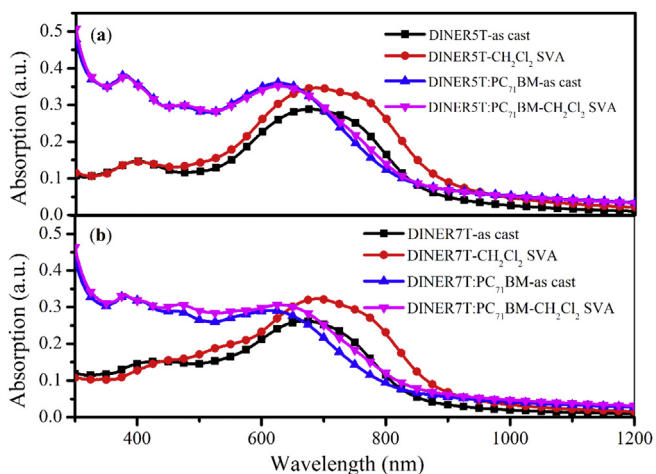


Fig. 3. Absorption spectra of **DINER5T** (a) and **DINER7T** (b) under different conditions.

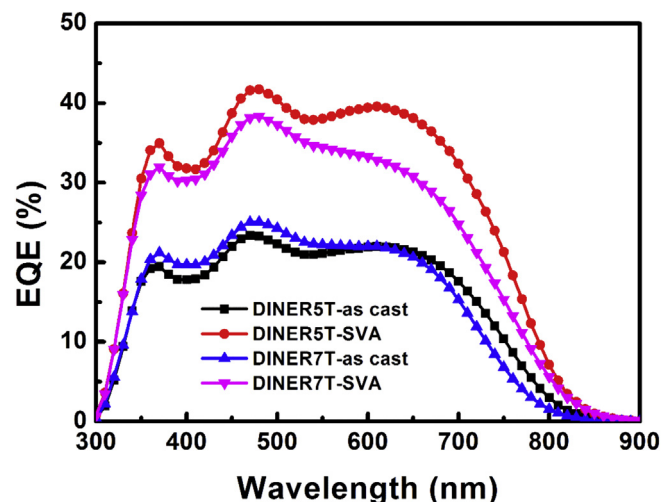


Fig. 4. EQE curves of **DINER5T** and **DINER7T** based devices under the conditions of as-cast and the SVA annealing with CH_2Cl_2 .

using the DFT method at the B3LYP/6.31G(d) level of theory to study the planarity of the two molecules. The optimized molecular geometries were shown in Fig. 6. From Fig. 6, it can be clearly seen that there exists an 8.99° and 9.15° dihedral angle between the plane of the end groups and the backbone of the molecules, respectively for **DINER5T** and **DINER7T**. Meanwhile, the **INER** unit is not a planar structure, and a $\sim 13^\circ$ dihedral angle exists between the plane of rhodanine and indaninone. This is contrary to the molecule **DRHD7T** and **DIN7T**, which all exhibit rather good planarity. This might be an important factor and making them have better performance.

4. Conclusion

In this work, a new end group **INER** was designed and synthesized based on two earlier end groups. Using this new end group, two new donor molecules, named **DINER5T** and **DINER7T**, were designed and synthesized. As expected, the absorption of both of the two molecules has a large red-shift of about 40–80 nm compared with the earlier oligothiophene based small donor molecules with rhodanine or indandione as the end groups. The two molecules showed low optical band gaps of 1.37 and 1.45 eV for **DINER5T** and **DINER7T**, respectively. OPV devices based on these two molecules were fabricated and optimized systematically. PCEs of 4.22% and 4.02% were achieved for **DINER5T** and **DINER7T** based devices, respectively. The moderate performances was attributed to the unsuitable phase separation scale as well as relatively poor planarity of the molecules, indicating a much balanced approach combing multi-factors need to be considered for high performance donor molecules.

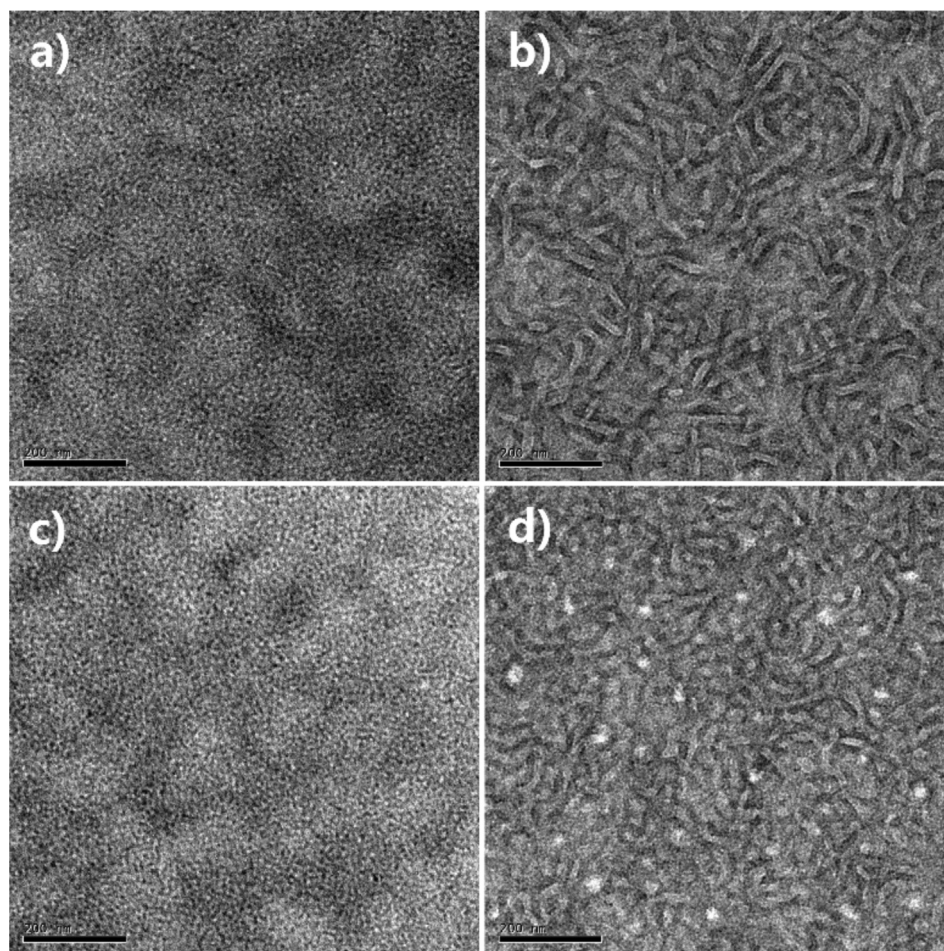


Fig. 5. TEM images of **DINER5T:PC₇₁BM** and **DINER7T:PC₇₁BM** blend films: a) and c) as cast blend films of **DINER5T:PC₇₁BM** and **DINER7T:PC₇₁BM** respectively, without SVA treatment; b) and d) **DINER5T:PC₇₁BM** and **DINER7T:PC₇₁BM** blend films with CH_2Cl_2 SVA for 60s.

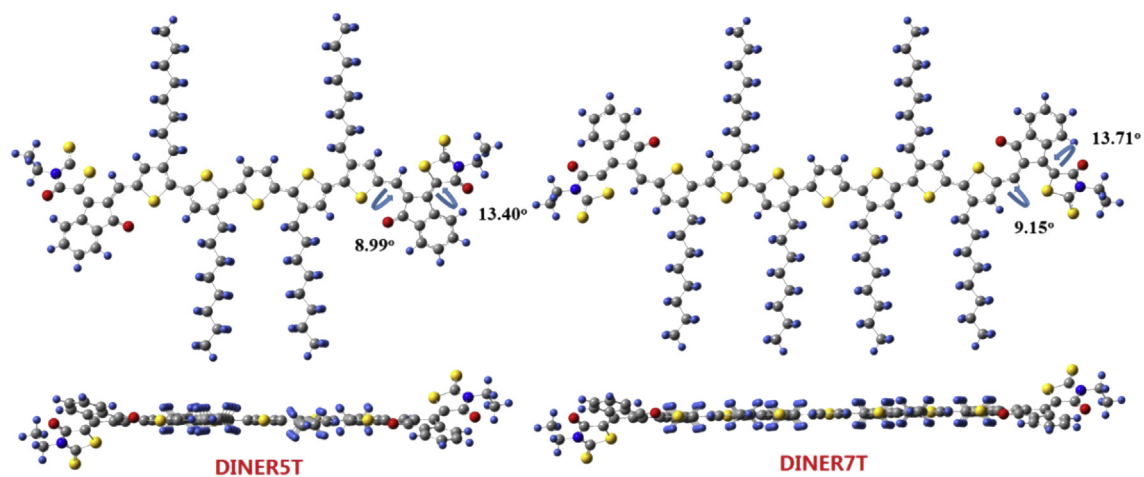


Fig. 6. Optimized molecular geometries for **DINER5T** and **DINER7T** applying DFT evaluated at the B3LYP/6.31G(d) level of theory.

Acknowledgment

The authors gratefully acknowledge the financial support from MoST (2014CB643502), NSFC (51373078, 51422304 and 91433101), PCSIRT (IRT1257) and Tianjin city (13RCFGX01121).

Appendix A. Supplementary data

Supplementary data related to this article can be found at <http://dx.doi.org/10.1016/j.orgel.2016.03.009>.

References

- [1] Y. Liu, J. Zhao, Z. Li, C. Mu, H. Hu, K. Jiang, H. Lin, H. Ade, H. Yan, *Nat. Comm.* 5 (2014) 5293.
- [2] H. Hu, K. Jiang, G. Yang, J. Liu, Z. Li, H. Lin, Y. Liu, J. Zhao, J. Zhang, F. Huang, Y. Qu, H. Yan, *J. Am. Chem. Soc.* 137 (2015), 14159–14157.
- [3] J. Kong, I. Hwang, K. Lee, *Adv. Mater.* 26 (2014) 6275–6283.
- [4] J. Chen, C. Cui, Y. Li, L. Zhou, Q. Ou, C. Li, Y. Li, J. Tang, *Adv. Mater.* 27 (2015) 1035–1041.
- [5] C. Liu, C. Yi, K. Wang, Y. Yang, R. Bhatta, M. Tsige, S. Xiao, X. Gong, *ACS Appl. Mater. Interface* 7 (2015) 4928–4935.
- [6] Z. He, B. Xiao, F. Liu, H. Wu, Y. Yang, S. Xiao, C. Wang, T.P. Russell, Y. Cao, *Nat. Phot.* 9 (2015) 174–179.
- [7] J. Kim, Z. Hong, G. Li, T. Song, J. Chey, Y. Lee, J. You, C. Chen, D.K. Sadana, Y. Yang, *Nat. Comm.* 6 (2015) 6391.
- [8] X. Ouyang, R. Peng, L. Ai, X. Zhang, Z. Ge, *Nat. Phot.* 9 (2015) 520–524.
- [9] J. Zhang, Y. Zhang, J. Fang, K. Lu, Z. Wang, W. Ma, Z. Wei, *J. Am. Chem. Soc.* 137 (2015) 8176–8183.
- [10] Q. Zhang, B. Kan, F. Liu, G. Long, X. Wan, X. Chen, Y. Zuo, W. Ni, H. Zhang, M. Li, Z. Hu, F. Huang, Y. Cao, Z. Liang, M. Zhang, T.P. Russell, Y. Chen, *Nat. Phot.* 9 (2015) 35–41.
- [11] B. Kan, Q. Zhang, M. Li, X. Wan, W. Ni, G. Long, Y. Wang, X. Yang, H. Feng, Y. Chen, *J. Am. Chem. Soc.* 136 (2014) 15529–15532.
- [12] B. Kan, M. Li, Q. Zhang, F. Liu, X. Wan, Y. Wang, W. Ni, G. Long, X. Yang, H. Feng, Y. Zuo, M. Zhang, F. Huang, Y. Cao, T.P. Russell, Y. Chen, *J. Am. Chem. Soc.* 137 (2015) 3886–3893.
- [13] W. Ma, C. Yang, X. Gong, K. Lee, A.J. Heeger, *Adv. Funct. Mater.* 15 (2005) 1617–1622.
- [14] G. Zhao, Y. Zhao, Y. Li, *Adv. Mater.* 22 (2010) 4355–4358.
- [15] B. Walker, A.B. Tamayo, X. Dang, P. Zalar, J.H. Seo, A. Garcia, M. Tantiwiwat, T.Q. Nguyen, *Adv. Funct. Mater.* 19 (2009) 3063–3069.
- [16] G. Li, Y. Yao, H. Yang, V. hrotriya, G. Yang, Y. Yang, *Adv. Funct. Mater.* 17 (2007) 1636–1644.
- [17] S. Miller, G. Fanchini, Y. Lin, C. Li, C. Chen, W. Su, M. Chhowalla, *J. Mater. Chem.* 18 (2008) 306–312.
- [18] M.C. Quiles, T. Ferenczi, T. Agostinell, P.G. Etchegin, Y. Kim, T.D. Anthopoulos, P.N. Stavrinou, D.D.C. Bradley, J. Nelson, *Nat. Mater.* 7 (2008) 158–164.
- [19] Y. Zhao, Z. Xie, Y. Qu, Y. Geng, L. Wang, *Appl. Phys. Lett.* 90 (2007) 043504.
- [20] J. Lee, W. Ma, C. Brabec, J. Yuen, J. Moon, J. Kim, K. Lee, G.C. Bazan, A.J. Heeger, *J. Am. Chem. Soc.* 130 (2008) 3619–3623.
- [21] Y. Yao, J. Hou, Z. Xu, G. Li, Y. Yang, *Adv. Funct. Mater.* 18 (2008) 1783–1789.
- [22] C. Hoven, X. Dang, R. Coffin, J. Peet, T.Q. Nguyen, G.C. Bazan, *Adv. Mater.* 22 (2010) E63–E66.
- [23] M. Su, C. Kuo, M. Yuan, U. Jeng, C. Su, K. Wei, *Adv. Mater.* 23 (2011) 3315–3319.
- [24] X. Guo, C. Cui, M. Zhang, L. Huo, Y. Huang, J. Hou, Y. Li, *Energy Environ. Sci.* 5 (2012) 7943–7949.
- [25] K. Wang, C. Yi, X. Hu, C. Liu, Y. Sun, J. Hou, Y. Li, J. Zheng, S. Chuang, A. Karim, X. Gong, *A.C.S. Appl. Mater. Interfaces* 6 (2014) 13201–13208.
- [26] F. Chen, J. Wu, C. Lee, Y. Hong, C. Kuo, M. Huang, *Appl. Phys. Lett.* 95 (2009) 013305.
- [27] E. Kymakis, G.D. Spyropoulos, R. Fernandes, G. Kakavelakis, A.G. Kanaras, E. Stratakis, *Acc. Phot.* 2 (2015) 714–723.
- [28] B. Yin, L. Yang, Y. Liu, Y. Chen, Q. Qi, F. Zhang, S. Yin, *Appl. Phys. Lett.* 97 (2010) 023303.
- [29] Y. Liu, X. Wan, F. Wang, J. Zhou, G. Long, J. Tian, J. You, Y. Yang, Y. Chen, *Adv. Energy. Matter* 1 (2011) 771–777.
- [30] K. Schulze, C. Uhrich, R. Schuppel, K. Leo, M. Pfeiffer, E. Brier, E. Reinold, P. Bauerle, *Adv. Mater.* 18 (2006) 2872–2875.
- [31] K. Hara, Z. Wang, T. Sato, A. Furube, R. Katoh, H. Sugihara, Y. Dan-oh, C. Kasada, A. Shinpo, S. Suga, *J. Phys. Chem. B* 109 (2005), 15476–154829.
- [32] M. Fischer, S. Wenger, M. Wang, A. Mishra, S. Zakeeruddin, M. Gratzel, P. Bauerle, *Chem. Matter* 22 (2010) 1836–1845.
- [33] L. Zheng, Y. Chung, Y. Ma, L. Zhang, L. Xiao, Z. Chen, S. Wang, B. Qu, Q. Gong, *Chem. Commun.* 50 (2014) 11196–11199.
- [34] Z. Li, J. Bian, Y. Wang, F. Jiang, G. Liang, P. He, Q. Hou, J. Tong, Y. Liang, Z. Zhong, Y. Zhou, W. Tian, *Sol. Energy Mater. Sol. Cells* 130 (2014) 336–346.
- [35] A. Tang, C. Zhan, J. Yao, *Chem. Mater.* 27 (2015) 4719–4730.
- [36] Y. Chen, X. Wan, G. Long, *Acc. Chem. Res.* 46 (2013) 2645–2655.
- [37] W. Ni, M. Li, X. Wan, Y. Zuo, B. Kan, H. Feng, Q. Zhang, Y. Chen, *Sci. China. Chem.* 58 (2015) 339–346.
- [38] Z. Li, G. He, X. Wan, Y. Liu, J. Zhou, G. Long, Y. Zuo, M. Zhang, Y. Chen, *Adv. Energy. Matter* 2 (2012) 74–77.
- [39] G. He, Z. Li, X. Wan, J. Zhou, G. Long, S. Zhang, M. Zhang, Y. Chen, *J. Mater. Chem. A* 1 (2013) 1801–1809.